https://doi.org/10.17221/133/2024-CJFS

Effects of hydroxyl radical oxidation on the structural and functional properties of mutton myosin

Yingying Cao, Huaiyu Li, Fubing Wang*

College of Life Science and Engineering, Lanzhou University of Technology, Lanzhou, China

**Corresponding author: cy_0533@126.com*

Citation: Cao Y., Li H., Wang F. (2024): Effects of hydroxyl radical oxidation on the structural and functional properties of mutton myosin. Czech J. Food Sci., 42: 423–434.

Abstract: To research the impact of free radical oxidation on myosin, we established a hydroxyl radical oxidation system using iron/hydrogen peroxide/ascorbic acid. By varying hydrogen peroxide concentrations (0, 0.5, 1, 5, 10, 20 mmol·L^{-1}), we achieved different oxidation levels of myosin and investigated the effects on its structural and functional characteristics. The results showed that when the H_2O_2 concentration was 20 mmol·L^{-1}, compared with the control group, the carbonyl content of myosin was 2.376 times higher, the sulfhydryl content was decreased by 37.02%, the surface hydrophobicity was increased by 59.13%, the solubility was decreased by 19.54%, and the turbidity was significantly increased ($P < 0.05$). Myosin emulsification, emulsification stability, and foaming capacity initially increased and then they diminished, and the maximum value was reached when the H_2O_2 concentration was 5 mmol·L^{-1}, whereas foaming stability remained relatively unchanged. Sodium dodecyl sulphate-polyacrylamide gel electrophoresis research revealed increased crosslinking and protein polymerisation in oxidised myosin. The secondary structure of myosin measured by Fourier infrared spectroscopy showed that the α-helix content decreased by 14.41% and the β-fold content increased by 44.50%. These results suggested that oxidative modification alters the structural and functional properties of myosin, providing valuable insights for its structural and functional analyses.

Keywords: SDS-PAGE; FTIR; oxidation of proteins; functional characteristics; structural characteristics

With the rapid development of the economy and society, and the acceleration of people's lifestyles, minced meat products (such as lunch meat, sausages, and meatballs) are becoming increasingly popular due to their convenience and high nutritional value. Consequently, consumer demands for the quality of minced meat products are also rising. Minced meat products, consisting of lean meat, fat, water, salt, and other additives, form a complex dispersed system (Ye et al. 2024). However, during their shelf life, these products often experience quality deterioration, which manifests like juice loss, surface drying, darkening of the meat filling, incomplete product integrity, cloudy cooking broth, frost on the product surface, development of an unpleasant rancid taste, increased losses upon thawing and cooking, and a decline in texture, hardness, elasticity, cohesiveness, and chewability. This significantly affects the consumer purchasing power and hinders the industrial, nutritional, and specialised development of minced meat products.

The formation of minced meat product quality is a process in which muscle proteins denature and

Supported by Project No. 32260553 of the National Natural Science Foundation of China.

https://doi.org/10.17221/133/2024-CJFS

coagulate to form a three-dimensional gel network structure (Zhu et al. 2021). The quality of minced meat products depends on the functional characteristics of muscle proteins, which directly influence the tissue state of the products, their water-holding capacity, emulsification, adhesiveness, and yield.

Protein oxidation is one of the most common chemical modifications of proteins. It involves the covalent modification of proteins through direct or indirect reactions with reactive oxygen species (ROS) and stress-related secondary products, leading to changes in the secondary and tertiary structures of proteins, thereby affecting their function and activity (Zhang et al. 2013). Excessive oxidation of myosin, particularly, alters protein conformation and secondary structures, significantly affecting processing characteristics and edible quality (Domínguez et al. 2021). Protein oxidation also affects the recognition of specific sites within protein structures by proteases, reducing enzymatic digestion efficiency and digestibility (Fu et al. 2019). Moreover, protein oxidation may increase cytotoxicity and mutagenicity, as modifications of L-phenylalanine by hydroxyl radicals can produce cytotoxic tyrosine, potentially causing protein synthesis disorders and triggering diseases (Gurer-Orhan et al. 2006). Protein oxidation directly leads to side-chain modifications, unfolding of structures, reduction in protein thiol content, increased carbonylation, protein crosslinking (disulphide and dityrosine bonding), reduced solubility, and decreased digestibility and functionality of proteins.

Numerous studies have demonstrated the impact of oxidation on protein structure (Lu et al. 2018; Jia et al. 2019). It has been found that mild oxidation can cause partial unfolding of myosin structure and increase the number of active sites for gel formation (Jiang et al. 2016). A 2019 study by Bhoke Marwa Nyaisaba examined the effects of hydroxyl radicals on the properties of myofibrillar proteins in fish meat. The study revealed that at higher concentrations of H_2O_2, total thiol groups were significantly reduced and carbonyl content increased; moderate concentrations (1 mmol·L^{-1}) of H_2O_2 enhanced the water-holding capacity and structural characteristics of the gel, while lower (0.1 mmol·L^{-1}) and higher (5, 10, and 20 mmol·L^{-1}) concentrations significantly reduced the water-holding capacity of the gel. Furthermore, sodium dodecyl sulfate-polyacrylamide gel electrophoresis (SDS-PAGE) and microscopic structural results confirmed that oxidation led to aggregation and denaturation of myofibrillar proteins, causing changes in the gelation structure of myofibrillar proteins; oxidation of myofibrillar proteins indicated that at moderate concentrations of oxidants, the structural properties of the heat gel were slightly improved (Nyaisaba et al. 2019). Therefore, controlling the degree of protein oxidation is crucial for controlling the quality of minced meat.

Mutton is one of the most popular foods worldwide, with China leading global production. Particularly, the northwestern region of China is a major source of high-quality mutton, known for its excellent water quality, abundant feed, and diverse animal breeds, resulting in juicy, tender, and flavourful meat that is renowned globally (Brand et al. 2018; Liu et al. 2019). Compared to other meat proteins such as pork and beef, mutton proteins exhibit significant differences: they are rich in branched-chain and other essential amino acids crucial for muscle synthesis and repair, and have a high biological utilisation rate. The unsaturated fatty acid content in mutton, especially ω-3 and ω-6 fatty acids, is relatively high, which benefits the cardiovascular health and also influences the oxidative sensitivity of mutton proteins.

Myofibrillar proteins (MPs) in mutton, accounting for 50–60% of the total protein content in meat, play a vital role in the quality of meat products (Guo et al. 2019). Myosin, a significant component of myofibrillar proteins, constitutes 50%~55% of myofibrillar proteins and one-third of the total protein in meat, participating in the formation process of meat gels and significantly influencing meat processing (Bayarsaikhan et al. 2019, Deng et al. 2021). Although nutritionally rich, mutton has poor protein stability; during storage, it is susceptible to oxidation by hydroxyl radicals due to processing and environmental factors. This oxidation gradually weakens gel structures, causing varying degrees of quality deterioration in minced meat as the protein oxidation process progresses (Tong et al. 2018). However, the causes of quality deterioration require further exploration; thus, this study uses mutton myosin as the subject, oxidising proteins with different concentrations of oxidants to investigate the mechanisms of oxidation.

MATERIAL AND METHODS

Fresh tenderloin (Tan Sheep, slaughtered within 12 h) from a vegetable market near Lanzhou University of Technology, Gansu Province. It was sealed, packed, and transported to the laboratory in an insulated container with ice packs. All other chemical reagents used were of analytical grade, and the experiments were conducted using distilled water.

https://doi.org/10.17221/133/2024-CJFS

Extraction and purification of myosin. Adapting the method proposed by Lei et al. (2022), fresh Tan Sheep tenderloin, devoid of fascia and fat, was chilled at 4 °C for 30 min, then minced using a meat grinder for 5 min. To this, thrice the volume of chilled extract A [0.5 mol·L^{-1} KCl, 0.1 mol·L^{-1} KH_2PO_4, 50 mmol·L^{-1} K_2HPO_4, 5.0 mmol·L^{-1} ethylenediamine tetraacetic acid (EDTA)-2Na, 4.0 mmol·L^{-1} sodium pyrophosphate, pH 6.5] was added and blended. The mixture was then homogenised in an ice bath at 5 000 × g for 5 min, followed by centrifugation (8 000 × g, 10 min, 4 °C) and filtration. The supernatant was diluted with a tenfold volume of pre-cooled water, mixed, and left to settle for 4 h at 4 °C before removing the supernatant and centrifuging the precipitate. Subsequently, thrice the volume of extract B (0.3 mol·L^{-1} KCl, 20 mmol·L^{-1} K_2HPO_4, 20 mmol·L^{-1} KH_2PO_4, pH 7.0) was added to the precipitate, stirred for 20 min, centrifuged at 8 000 × g for 10 min at 4 °C, and the supernatant was combined with a tenfold volume of pre-cooled water. After another centrifugation, the precipitate was dissolved in an equivalent volume of dialysate (0.6 mol·L^{-1} KCl, 20 mmol·L^{-1} K_2HPO_4, 20 mmol·L^{-1} KH_2PO_4, pH 7.5). Dialysis was performed in a dialysis bag (10 000 Da) for 24 h to obtain the myosin solution, followed by a final centrifugation (10 000 × g, 10 min, 4 °C) to remove the supernatant. Protein content was quantified using the biuret method, and myosin purity was evaluated using SDS-PAGE.

Oxidation of myosin. Following a slight modification of the method (Zhang et al. 2020), myosin concentration was adjusted to 20 mg·mL^{-1} using a phosphate buffer (50 mmol·L^{-1} KH_2PO_4, 50 mmol·L^{-1} K_2HPO_4, 0.6 mol·L^{-1} KCl, pH 6.5). Equal volumes of myosin solution and oxidation system [comprising 0.1 mmol·L^{-1} ferric chloride, 1 mmol·L^{-1} ascorbic acid, and varying H_2O_2 concentrations (0, 0.5, 1, 5, 10, 20 mmol·L^{-1})] were mixed. Oxidation proceeded in darkness at 4 °C for 24 h, halted by adding 1 mmol·L^{-1} EDTA. A double volume of phosphate buffer was added, followed by centrifugation (8 000 × g, 4 °C, 10 min). The precipitate was washed twice with the same buffer and centrifuged under identical conditions. Finally, the precipitate was redissolved in phosphate-buffered saline (PBS, 20 mmol·L^{-1} KH_2PO_4, 20 mmol·L^{-1} K_2HPO_4, 0.6 mol·L^{-1} KCl, pH 6.5) buffer and stored at 4 °C.

Determination of carbonyl content. Adapting the method (Chen et al. 2023), the myosin concentration was adjusted to 5 mg·mL^{-1} in PBS buffer. In a 5 mL centrifuge tube, 0.8 mL of myosin solution was combined with 1 600 µL of 2 mol·L^{-1} HCl solution and reacted at room temperature for 30 min. Subsequently, 800 µL of trichloroacetic acid (0.4 g·mL^{-1}) was added, followed by centrifugation to discard the precipitate. The precipitate was washed thrice, then redissolved in 3 mL of phosphate buffer. After resting for 12 h, absorbance at 370 nm was measured. Carbonyl content was calculated using the molar extinction coefficient (22 000 M^{-1}·cm^{-1}) as shown in Equation 1.

$$\textit{Carbonyl group content}\ \left(\text{nmol·mg}^{-1}\right) = \frac{A}{22\,000 \times C} \times 10^6 \quad (1)$$

where: A – absorbance at 370 nm; C – concentration of the protein sample (mg·mL^{-1}).

Determination of sulfhydryl content. Adapting the method from Xinrong et al. (2023) with slight modifications, the myosin concentration was adjusted to 5 mg·mL^{-1} in PBS buffer. We mixed 1 mL of this protein solution with 9 mL of phosphate buffer. In a test tube, 3 mL of this diluent and 0.4 mL of 0.1% 5,5'-dithiobis(2-nitrobenzoic acid) were combined and reacted at 40 °C in the dark for 30 min. After cooling to room temperature, the absorbance at 412 nm was measured. The sulfhydryl content was calculated using the molar extinction coefficient (13 600 M^{-1}·cm^{-1}), as illustrated in Equation 2.

$$\textit{Sulfhydryl group content}\ \left(\text{nmol·mg}^{-1}\right) = \frac{A \times 10^5}{136 \times C} \quad (2)$$

where: A – absorbance at 412 nm.

Determination of surface hydrophobicity. Following minor modifications to the method (Yantao et al. 2023), the myosin concentration was adjusted to 5 mg·mL^{-1} in PBS buffer. To a 2 mL centrifuge tube, we added 1 mL of the sample solution (5 mg·mL^{-1}) and 200 µL of bromophenol blue (BPB) solution (1 mg·mL^{-1}), mixing for 10 min. After centrifugation, absorbance was measured at 595 nm with a 10-fold dilution. Surface hydrophobicity was determined using Equation 3.

$$\text{BPB}\ \textit{combining weight}\ \left(\mu\text{g}\right) = \frac{A_0 - A_1}{A_0} \times 200 \quad (3)$$

where: BPB – bromophenol blue; A_0 – absorbance of the blank sample at 595 nm; A_1 – absorbance of the sample at 595 nm.

https://doi.org/10.17221/133/2024-CJFS

Determination of solubility. Adapting the methodology from Ge et al. (2022), myosin samples were concentrated to 2.5 mg·mL^{-1} in PBS buffer, incubated at 4 °C for 1 h, and then centrifuged (8 000 × g, 4 °C, 20 min) to separate the supernatants. The solubility was evaluated by comparing the concentration of myosin solution before and after centrifugation (C_0 and C_1), as described in Equation 4.

$$Solubility\ (\%) = \frac{C_1}{C_0} \times 100 \quad (4)$$

where: C_0 – concentration of myosin solution before centrifugation; C_1 – concentration of myosin solution after centrifugation.

Determination of turbidity. Following the procedure by Shui et al. (2024), the myosin concentration in PBS buffer was adjusted to 1 mg·mL^{-1}. The sample solution (5 mL) was heated to 50 °C and 80 °C for 30 min each. After cooling and resting for 1 h, the solution absorbance at 600 nm was measured to determine turbidity, which is given as $A_{600\,nm}$.

Determination of foaming and foam stability. In accordance with the method outlined by Haihua et al. (2023), the myosin concentration was adjusted to 5 mg·mL^{-1} with PBS buffer. A 10 mL aliquot of the solution was placed in a 50 mL plastic measuring cylinder [initial volume V_0 (mL)] and agitated at 2 000 × g at 25 °C for 1 min. The immediate foam volume was noted as V_1 (mL). After an hour, the foam volume [V_t (mL)] was measured again. Foaming capacity (F_c) and foam stability (F_s) were calculated using Equations 5 and 6, respectively:

$$F_c\ (\%) = \frac{V_1 - V_0}{V_0} \times 100 \quad (5)$$

$$F_s\ (\%) = \frac{V_t}{V_1} \times 100 \quad (6)$$

where: F_c – foaming capacity; V_0 – initial volume (mL); V_1 – immediate foam volume (mL); V_t – foam volume (mL); F_s – foam stability.

Determination of emulsifying properties. Following the method proposed by Wu et al. (2023), the myosin concentration was set to 5 mg·mL^{-1} in PBS buffer. In a 50 mL centrifuge tube, 2.0 mL of soybean oil and 8.0 mL of the sample solution were combined, thoroughly mixed, and then 50 µL of the emulsion, extracted 0.5 cm above the tube base, was added to 5 mL of 0.1% SDS solution. The mixture was shaken and the absorbance (A_1) was measured at 500 nm. After a 10-min stand, the procedure was repeated to determine the absorbance (A_2), using 0.1% SDS solution as the blank control. The emulsifying activity index (*EA*I) and emulsion stability index (*ESI*) were calculated using Equations 7 and 8, respectively:

$$EAI\ \left(m^2 \cdot g^{-1}\right) = \frac{2 \times 2.303 \times A_1 \times 500}{\rho \times \left(1 - \varphi\right) \times 10^4} \quad (7)$$

$$ESI\ (\%) = \frac{A_2}{A_1} \times 100 \quad (8)$$

where: *EAI* – emulsifying activity index; *ESI* – emulsion stability index; ρ – mass concentration of MP (g·mL^{-1}); ϕ – volume fraction of oil phase (20%); A_1 and A_2 – absorbance of the emulsion at 0 and 10 min, respectively.

Sodium dodecyl sulfate-polyacrylamide gel electrophoresis. Adapting the technique from Shen Hui et al. (Shen et al. 2020), for SDS-PAGE analysis 5% stacking gel and 12% resolving gel were used. Each lane was loaded with 10 µL of 1 mg·mL^{-1} sample solution. The electrophoresis was conducted at 75 V for stacking and 120 V for resolving. After electrophoresis, the gel was stained with Coomassie brilliant blue, destained, and then imaged using a gel documentation system.

Fourier transformed infrared spectroscopy. Following the procedure described by Juanjuan et al. (2022), a 1 mg lyophilised protein sample was blended with 100 mg KBr, ground, and compressed into pellets. The fourier transformed infrared spectroscopy (FTIR) spectra were recorded at room temperature across a range of 400 to 4 000 cm^{-1}. Peak Fit software (version 4.0), which uses a Gaussian peak fitting algorithm, was used to investigate the secondary structure of myosins.

Data analysis. Each experimental condition was replicated thrice, with results presented as mean ± standard deviation. GraphPad Prism software (version 8) facilitated the analysis of variance and significance testing, where $P < 0.05$ was considered statistically significant. Omnic (version 9.2) and Peak Fit (version 4.12) were used for secondary structure analysis, while GraphPad Prism (version 8) supported correlation analysis and graphical presentations.

https://doi.org/10.17221/133/2024-CJFS

RESULTS AND DISCUSSION

Effects of different oxidation levels on the carbonyl content of mutton myosin. Protein carbonyls, as primary oxidation products in meat during storage, signify crucial chemical modifications in oxidised proteins (Christina et al. 2023). As depicted in Figure 1, the carbonyl content escalates markedly with increasing H_2O_2 concentration ($P < 0.05$), which indicates increased oxidation. The control group exhibited a carbonyl content of 1.982 nmol·mg^{-1}; when the concentration of H_2O_2 was 5, 10, and 20 mmol·L^{-1}, the carbonyl content was 3.244, 4.292, and 4.711 nmol·mg^{-1}, respectively. The concentration of H_2O_2 increased significantly at 10 mmol·L^{-1}, which was 2.165 times higher than that of the control group. When the concentration of H_2O_2 was 20 mmol·L^{-1}, it increased 2.376 times compared with that of the control group, and the increase was slower; it was estimated that when the concentration of H_2O_2 was greater than 10 mmol·L^{-1}, the protein was almost completely oxidised. Reactive oxygen species target peptide bonds or side chain groups, causing oxidation and formation of carbonyl derivatives (Márquez-Lázaro et al. 2022, Ramadhan et al. 2024).

Effects of different oxidation levels on the sulfhydryl content in mutton myosin. The reduction in sulfhydryl groups is a prevalent characteristic of protein alterations under oxidative stress (Lepedda and Formato 2020). Figure 2 illustrates a significant decline in sulfhydryl content with increasing H_2O_2 concentration ($P < 0.05$). When the concentration of H_2O_2 was 5, 10, and 20 mmol·L^{-1}, the sulfhydryl content was 42.25, 39.69, and 31.19 nmol·mg^{-1}, respectively. When the concentration of H_2O_2 increased to 20 mmol·L^{-1}, the sulfhydryl content decreased to 31.19 nmol·mg^{-1}, which was 37.02% lower than that of the control group. This trend also indicates that the degree of protein oxidation is deepening, which corresponds to the trend of carbonyl change. This reduction occurs as myosin sulfhydryl groups are vulnerable to attack by reactive oxygen species, leading to their conversion into disulphide bonds, sulphenic acid, sulphonic acid, or nitrosothiol formation through interaction with nitric oxide. Additionally, the decline in sulfhydryl content may result from the extensive exposure of internal sulfhydryl groups (-SH) in myosin due to OH radical oxidation and the subsequent capture of hydrogen atoms from sulphur-containing amino acid (cysteine) residues (Soladoye et al. 2015, Ramadhan et al. 2024).

Effects of different degrees of oxidation on the surface hydrophobicity of mutton myosin. Surface hydrophobicity, indicating the presence of hydrophobic amino acids on the protein surface, serves as a marker for protein conformational changes (Cheng et al. 2023). Figure 3 demonstrates that the my-

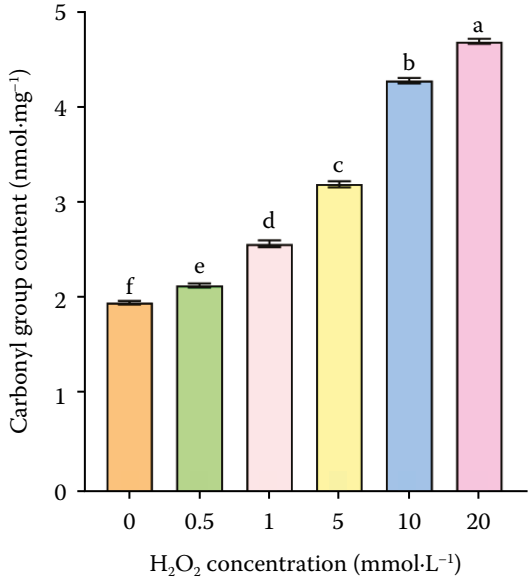

Figure 1. Effect of hydroxyl radical oxidation on carbonyl content in mutton myosin

a–f – different letters indicate significant difference in H_2O_2 concentration ($P < 0.05$)

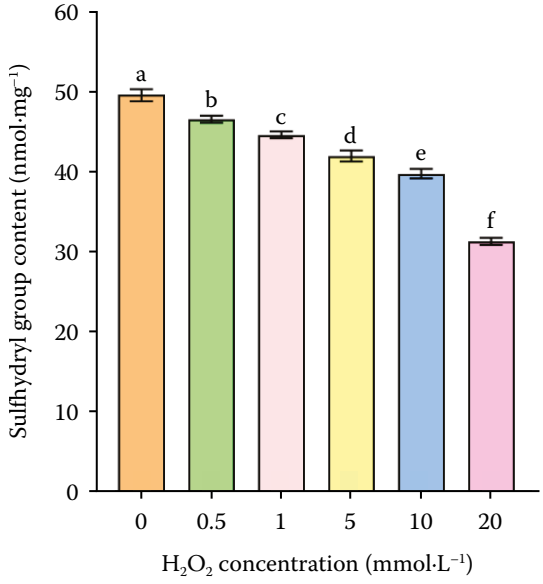

Figure 2. Changes in sulfhydryl content in mutton myosin after hydroxyl radical oxidation

a–f – different letters indicate significant difference in H_2O_2 concentration ($P < 0.05$)

https://doi.org/10.17221/133/2024-CJFS

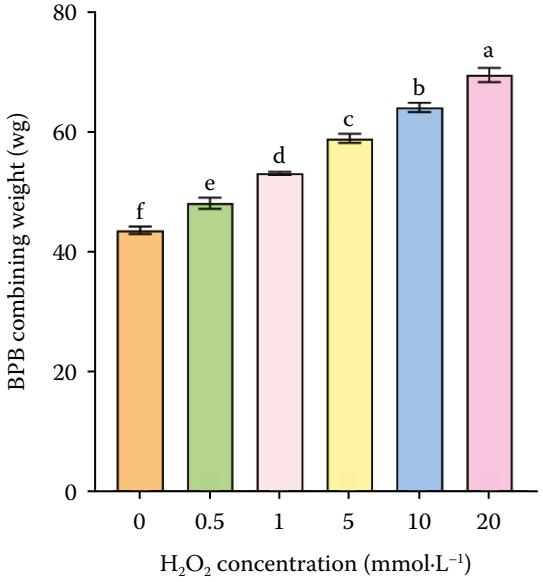

Figure 3. Changes in the surface hydrophobicity of mutton myosin after oxidation by hydroxyl radicals

a–f – different letters indicate significant difference in H_2O_2 concentration ($P < 0.05$); BPB – bromophenol blue

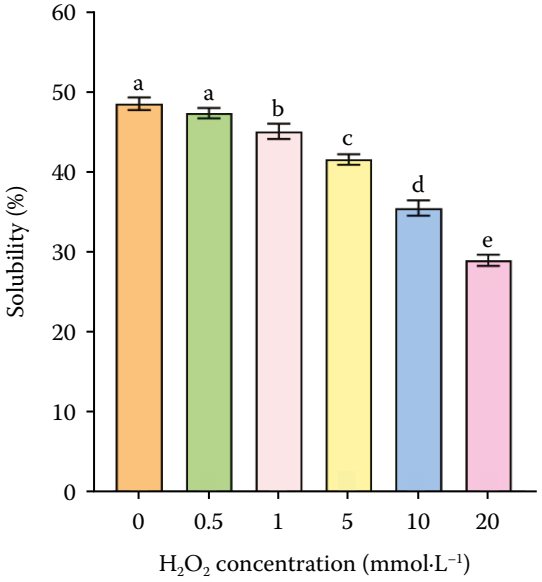

Figure 4. Changes in the solubility of mutton myosin after hydroxyl radical oxidation

a–e – different letters indicate significant difference in H_2O_2 concentration ($P < 0.05$)

osin surface hydrophobicity increases with the rising H_2O_2 concentration ($P < 0.05$). In the control group, the bromophenol blue binding amount was 43.65 μg, which surged to 69.46 μg at 20 mmol·L^{-1} H_2O_2, which was a 59.13% increase compared to the control. This rise may stem from alterations in protein structure and conformation under intense oxidation, exposing numerous hydrophobic groups and elevating the surface hydrophobicity. It could also relate to protein aggregation, which might shield unfolding proteins under strong oxidation, with protein refolding due to aggregation and multimer formation further augmenting the surface hydrophobicity (Xu et al. 2020).

Effects of different degrees of oxidation on the solubility of mutton myosin. Solubility is indicative of protein aggregation and crosslinking levels and serves as a key parameter in assessing protein characteristics (Malik et al. 2017). As depicted in Figure 4, myosin solubility diminishes markedly with an increase in H_2O_2 concentration ($P < 0.05$). The solubility dropped from 48.64% to 29.10% as H_2O_2 concentration escalated from 0 mmol·L^{-1} to 20 mmol·L^{-1}, which was a 19.54% reduction compared to the control. This decrease after oxidation treatment likely stems from alterations in protein molecule conformation, leading to the formation of insoluble aggregates and the correlation between higher oxidation and lower solubility. Additionally, extensive oxidation may cause protein denaturation and precipitation, thereby diminishing solubility. Insoluble aggregates emerge from the covalent crosslinking of protein molecules, which compromises solubility. The interaction of proteins with peroxides alters the protein energy state, inducing denaturation and ultimately reducing solubility (Zhou and Yang 2020).

Effects of different degrees of oxidation on the turbidity of mutton myosin. Turbidity measures the obstruction of light transmission through a solution and is used to gauge the protein aggregation (Kong et al. 2023), indirectly reflecting solubility changes. This study used the absorbance at 600 nm as a turbidity metric. Figure 5 illustrates a significant increase in turbidity alongside the rising H_2O_2 concentration ($P < 0.05$). This effect is attributed to oxidation-induced crosslinking and aggregation of protein molecules, decreasing solubility and enhancing turbidity. The turbidity outcomes align with solubility observations, underscoring that oxidation promotes the protein molecule aggregation, leading to reduced solubility.

Effects of different oxidation degrees on foaming capacity and foam stability of mutton myosin. The foaming capacity of proteins contributes to the airy structure and pleasant taste of food, which is associated with the content of soluble protein and its stability in solution (Jin et al. 2022). As depicted in Figure 6A, the foaming property of the

https://doi.org/10.17221/133/2024-CJFS

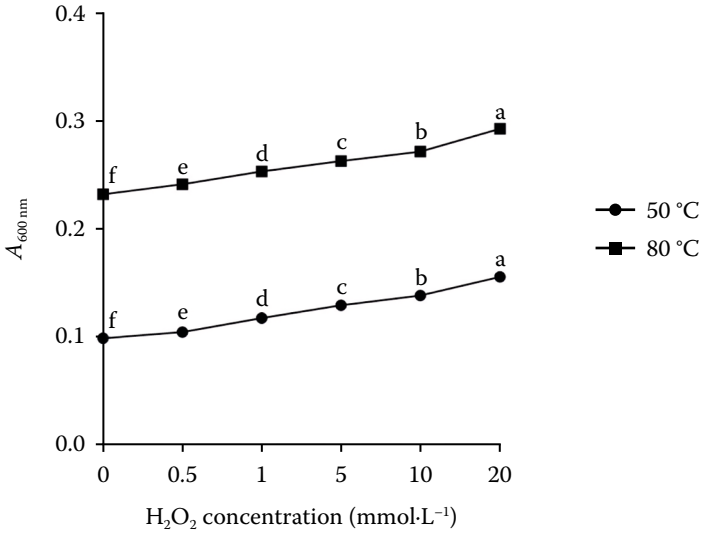

Figure 5. Changes in mutton myosin turbidity after hydroxyl radical oxidation

a–f – different letters indicate significant difference in H_2O_2 concentration ($P < 0.05$); $A_{600\ nm}$ – absorbance at 600 nm

control group was 17%, and when the concentration of H_2O_2 was 5 mmol·L^{-1} and 20 mmol·L^{-1}, the foaming property was 48% and 38%, respectively. The foaming capacity of myosin initially increased and then it decreased, and the foaming property reached the maximum value when the H_2O_2 concentration was 5 mmol·L^{-1}; the foaming performance began to decrease as the H_2O_2 concentration continued to increase, but it was still higher than that of the control group, so it was obvious that oxidation was beneficial to the foaming property of myosin. This could be due to hydroxyl radical oxidation causing the partial unfolding of protein molecules, exposing internal hydrophobic residues, and facilitating rapid adsorption at the two-phase interface, thereby enhancing foaming. However, as oxidation progresses, sulfhydryl groups oxidise to form disulphide bonds, and larger crosslinks create insoluble aggregates like protein polymers, increasing the interfacial tension. Additionally, reduced solubility diminishes the available protein content for foam formation, leading to decreased foamability (Duan et al. 2018). The myosin foam stability showed minor changes (Figure 6B), with oxidation not significantly affecting it, maintaining over 80% stability.

Effects of different degrees of oxidation on emulsifying properties of mutton myosin. Emulsifying

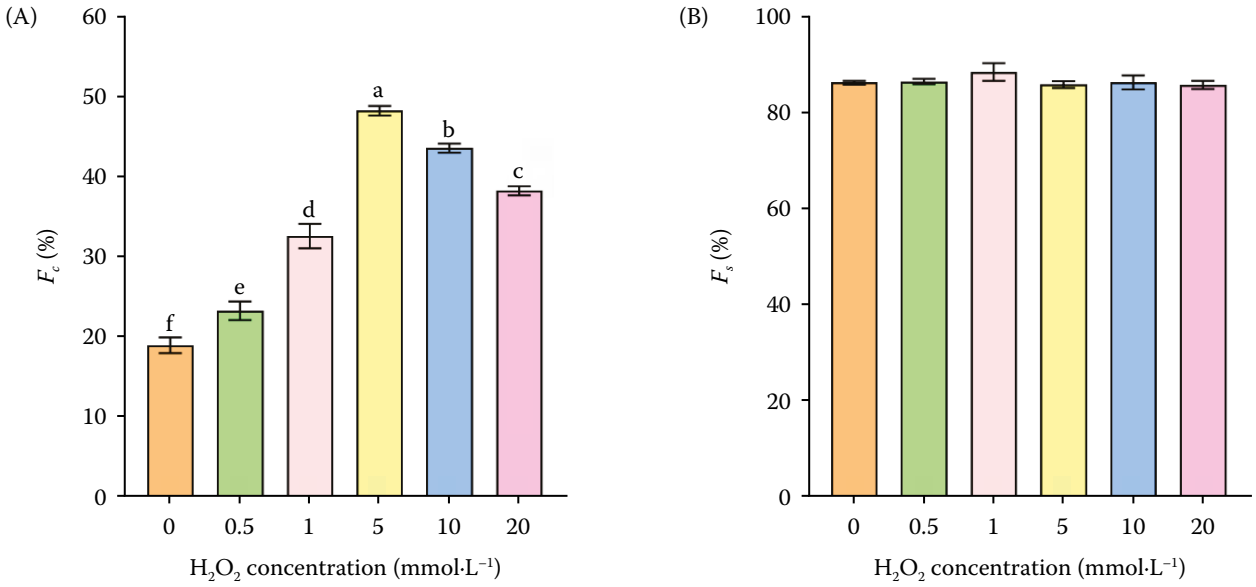

Figure 6. Changes in myosin (A) foaming capacity and (B) foam stability after oxidation

a–f – different letters indicate significant difference in H_2O_2 concentration ($P < 0.05$); F_c – foaming capacity; F_s – foam stability

https://doi.org/10.17221/133/2024-CJFS

properties are the protein capacity to form emulsions with oil and water in a food system, assessed by emulsifying ability and stability (Cao et al. 2022). Figure 7 illustrates that the emulsification of the control group was 18.45 $m^2 \cdot g^{-1}$, and the emulsification of H_2O_2 was 21.22, 18.15 , and 16.02 $m^2 \cdot g^{-1}$ when the concentrations of H_2O_2 were 5, 10, and 20 $mmol \cdot L^{-1}$, respectively. At low H_2O_2 concentrations, myosin emulsification significantly increased with rising H_2O_2 levels ($P < 0.05$). However, as H_2O_2 concentration further increased, emulsification began to decline, dropping below control levels at 20 $mmol \cdot L^{-1}$ H_2O_2. Additionally, the emulsion stability of the control group (0 $mmol \cdot L^{-1}$ H_2O_2) was 46.06%, the emulsion stability index (*ESI*) of myosin first rose and then it fell, peaking at an H_2O_2 concentration of 1 $mmol \cdot L^{-1}$. Beyond this point, *ESI* significantly decreased, falling below control levels. Therefore, it is speculated that moderate oxidation is beneficial to the emulsification and emulsion stability of myosin, while excessive oxidation will destroy its emulsification and emulsion stability. These findings align with those of Chen et al. (2020), suggesting that an overly oxidative environment can induce protein conformational changes and crosslink formation, oxidative muscle damage, and impact water retention and emulsifying properties.

SDS-PAGE analysis. The impact of oxidation on myosin was assessed using reductive (+βME) SDS-PAGE. In Figure 8 the myosin heavy chain (MHC, about 240 kDa) is at the top of the band when the myosin heavy chain (MHC 240 kDa) was the main component of myosin (Potter 2022). In addition to the myosin heavy chain, three myosin light chains were found in the low intensity band, namely light chain 1 (MYL1, about 17 kDa), light chain 2 (MYL1, about 14 kDa) and light chain 3 (MYL1, about 21 kDa). With the increase of H_2O_2 concentration, the grey levels of both the myosin heavy chain band and the myosin light chain band gradually become lighter, which may be caused by hydroxyl radicals attacking the heavy chain and the light chain of myosin, destroying the disulphide bond in them and causing the oxidative degradation of myosin, thus leading to the lightening of the heavy chain and light chain bands. When H_2O_2 concentration is 10 M and 20 M, a new band A with molecular weight of about 100 kDa appears, while no new band is generated at 0.5, 1, and 5 M. The generation of band A may be related to the aggregation produced by disulphide bond crosslinking during the oxidation of myosin. In mild oxidation, myosin may not crosslink or crosslink is not obvious, and it is easy to be destroyed and recovered. In the case of severe oxidation, myosin is prone to crosslinking to produce new aggregates, and this change is irreversible; the aggregation becomes more obvious with the increase of the oxidation degree. This corresponds to the results before turbidity increase and solubility decrease at 10 M and 20 M. Li's experiment showed that the protein crosslinking phe-

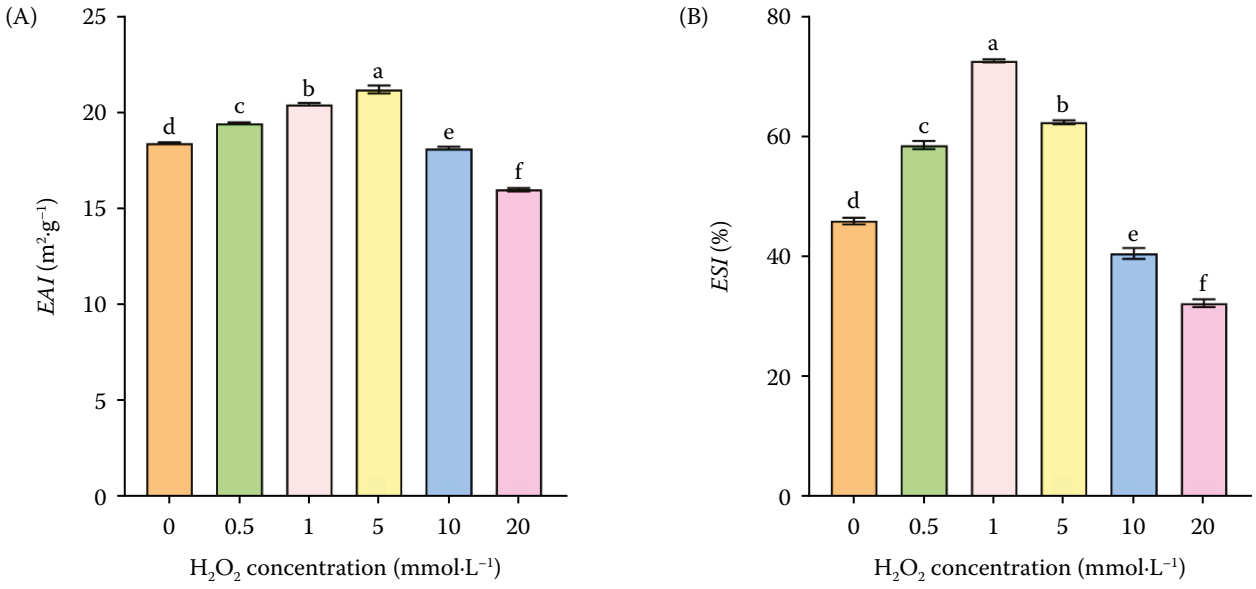

Figure 7. Changes in the (A) emulsification and (B) emulsification stability of myosin after oxidation

a–f – different letters indicate significant difference in H_2O_2 concentration ($P < 0.05$); *EAI* – emulsifying activity index; *ESI* – emulsion stability index

https://doi.org/10.17221/133/2024-CJFS

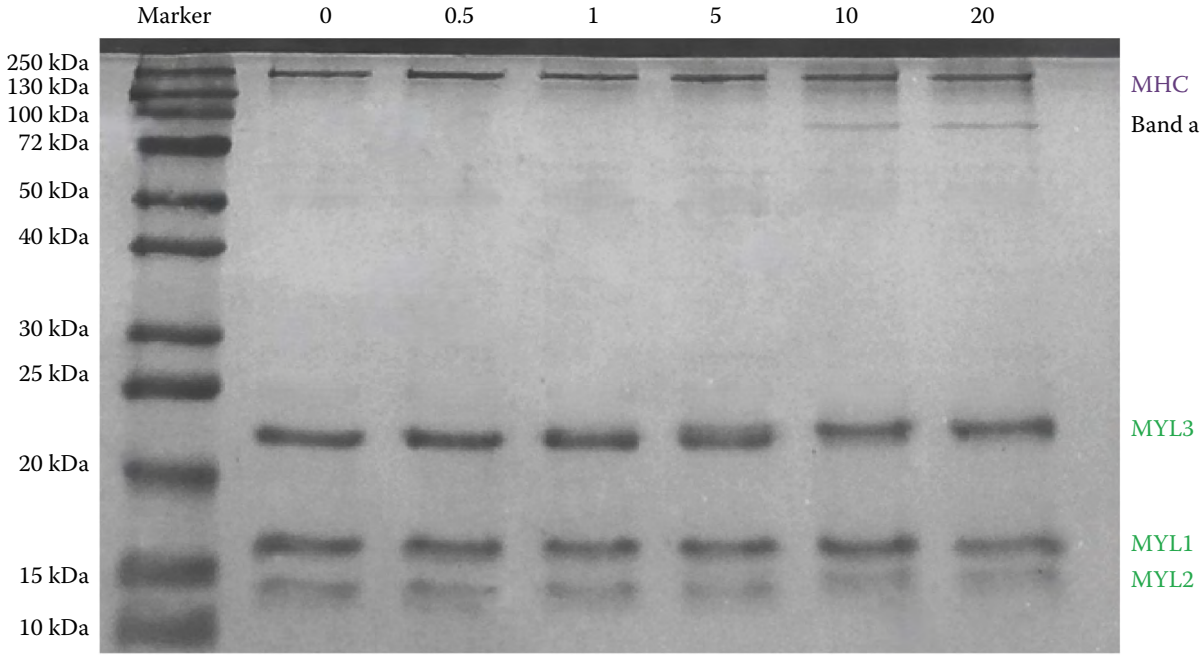

Figure 8. Sodium dodecyl sulfate-polyacrylamide gel electrophoresis (SDS-PAGE) diagram of the myosin globulin after hydroxyl radical oxidation

MHC – myosin heavy chain; MYL – myosin light chain

nomenon also occurred under irradiation induction (Li et al. 2018).

Fourier transformed infrared spectroscopy spectrum analysis. The secondary structure, indicative of the protein spatial conformation, can be analysed using the amide I band (1 600–1 700 cm^{-1}) (Menard et al. 2021). Figure 9 illustrates the FTIR spectra of myosin after hydroxyl radical oxidation. Figure 10 reveals post-oxidation alterations in the secondary structure components of myosin. Relative to the control

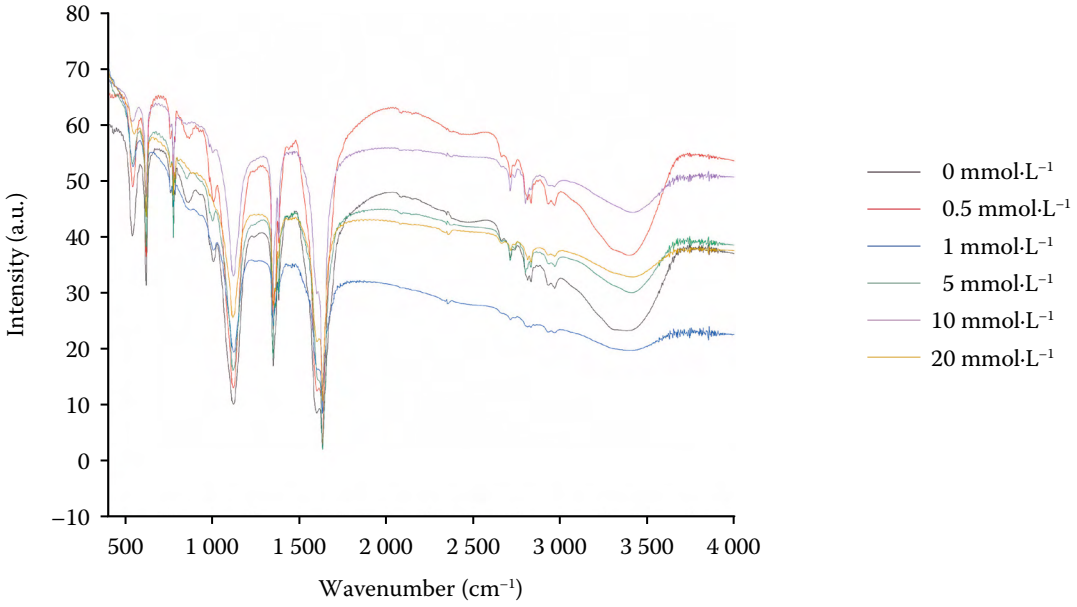

Figure 9. Fourier transformed infrared spectroscopy (FTIR) profile of myosin after hydroxyl radical oxidation

a.u. – absorbance unit

https://doi.org/10.17221/133/2024-CJFS

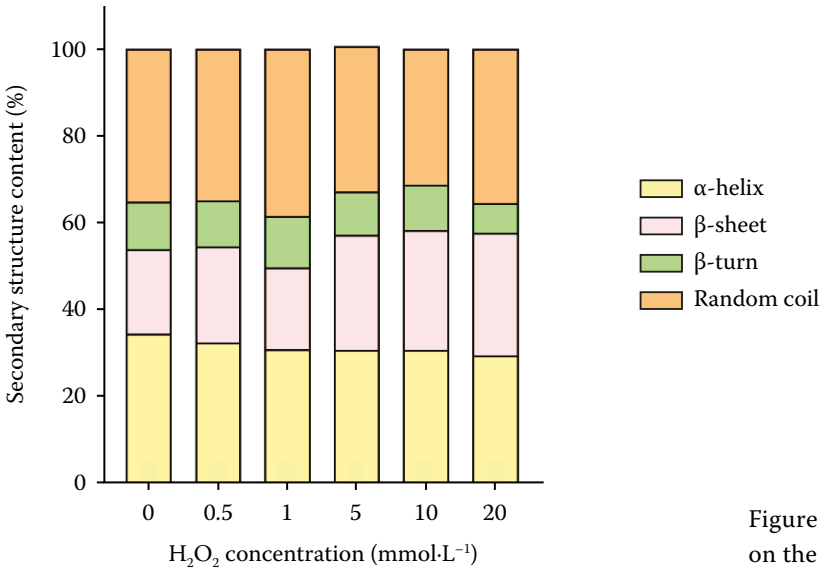

Figure 10. Effect of hydroxyl radical oxidation on the secondary structure of mutton myosin

(0 mmol·L^{-1} H_2O_2), oxidation diminished the α-helix proportion, increased the β-sheet content, and reduced the β-turn presence. It is well known that the secondary structure of proteins is determined by hydrogen bonds and electrostatic interactions between amino acids (Yu et al. 2023). Thus, hydroxyl radicals may attack the cysteine of the myosin head first, leading to progressive unfolding of the S1 subunit of the head, causing a change in the myosin conformation that results in the instability of the α-helix and, consequently, in reduction. Intermolecular hydrogen bonding between carbonyl (C = O) and amino (N-H) groups on polypeptide chains and adjacent chains escalates, boosting the β-sheet content. As the H_2O_2 concentration climbs, further structural unfolding occurs, with sulfhydryl groups oxidising into disulphide bonds, causing peptide chains to refold, increasing the β-turn content. These findings align with the observations made by Zhang et al. (2019), where an increase in β-sheet content corresponded with a decrease in α-helices, β-turns, and random coils with escalating oxidant levels.

CONCLUSION

This study employed varying concentrations of hydroxyl radicals to oxidise mutton myosin, investigating their impact on the physicochemical and structural properties of the protein. As the concentration of H_2O_2 solution increased, a rise in carbonyl content and a decline in thiol content were observed, accompanied by an increase in surface hydrophobicity. Fourier-transform infrared spectroscopy of the secondary structure of myosin indicated a gradual decrease in α-helix content, an increasing trend in β-sheet content, and a rise in random coil content, suggesting a transition from ordered to disordered protein structures. With the progression of oxidation, at a concentration of 5 mmol·L^{-1}, an increase in protein foamability and emulsifying properties was noted, suggesting that moderate oxidation enhances the functional properties of the protein. However, at concentrations of 10 mmol·L^{-1} and 20 mmol·L^{-1}, significant reductions in protein foamability and emulsifying properties were observed, and SDS-PAGE revealed the appearance of new bands, likely related to aggregates formed by disulphide bond crosslinking during the oxidation process. This corresponds with increased turbidity and decreased solubility at concentrations of 10 mmol·L^{-1} and 20 mmol·L^{-1}. Hence, it is hypothesised that at concentrations greater than 10 mmol·L^{-1}, nearly complete oxidation occurs, leading to increased protein crosslinking and a consequent decline in protein functional properties.

REFERENCES

Bayarsaikhan G., Avan A.N., Çekiç S.D., Apak R. (2019): Use of modified CUPRAC and dinitrophenylhydrazine colorimetric methods for simultaneous measurement of oxidative protein damage and antioxidant defense against oxidation. Talanta, 204: 613–625.

Brand T.S., Van Der Merwe D.A., Hoffman L.C., Geldenhuys G. (2018): The effect of dietary energy content on quality characteristics of Boer goat meat. Meat Science, 139: 74–81.

Cao Y., Li Z., Fan X., Liu M., Han X., Huang J., Xiong Y.L. (2022): Multifaceted functionality of l-arginine in modu-

https://doi.org/10.17221/133/2024-CJFS

lating the emulsifying properties of pea protein isolate and the oxidation stability of its emulsions. Food & Function, 13: 1336–1347.

Chen J., Zhang X., Xue S., Xu X. (2020): Effects of ultrasound frequency mode on myofibrillar protein structure and emulsifying properties. International Journal of Biological Macromolecules, 163: 1768–1779.

Chen M., Pan Q., Wu B., Wang H., Yi Y., Xu W., Guo D. (2023): Effect of fenugreek (*Trigonella foenum-graecum* L.) seed extracts on the structure of myofibrillar protein oxidation in duck meat. Foods, 12: 4482.

Cheng J.H., Li J., Sun D.W. (2023): Effects of dielectric barrier discharge cold plasma on structure, surface hydrophobicity and allergenic properties of shrimp tropomyosin. Food Chemistry, 409: 135316.

Christina B., Baikuntha A., Ashutosh R.V. (2023): Divalent ions as mediators of carbonylation in cardiac myosin binding protein C. Journal of Molecular Graphics and Modelling, 124: 108576.

Deng X., Lei Y., Liu J., Lu S., Zhang J. (2021): Effect of oxidation on the structural and functional properties of myofibrillar in Coregonus peled. International Food Research Journal, 28: 960–968.

Domínguez R., Pateiro M., Munekata P.E.S., Zhang W., Garcia-Oliveira P., Carpena M., Prieto M.A., Bohrer B., Lorenzo J.M. (2021): Protein oxidation in muscle foods: A comprehensive review. Antioxidants, 11: 60.

Duan X., Li M., Shao J., Chen H., Xu X., Jin Z., Liu X. (2018): Effect of oxidative modification on structural and foaming properties of egg white protein. Food Hydrocolloids, 75: 223–228.

Fu Q., Liu R., Wang H., Hua C., Song S., Zhou G., Zhang W. (2019): Effects of oxidation *in vitro* on structures and functions of myofibrillar protein from beef muscles. Journal of Agricultural and Food Chemistry, 67: 5866–5873.

Ge H., Jianhang X., Qian C., Xiufang X., Haotian L., Baohua K. (2022): Improving the solubility of myofibrillar proteins in water by destroying and suppressing myosin molecular assembly via glycation. Food Chemistry, 395: 133590.

Guo Z., Li Z., Wang J., Zheng B. (2019): Gelation properties and thermal gelling mechanism of golden threadfin bream myosin containing $CaCl_2$ induced by high pressure processing. Food Hydrocolloids, 95: 43–52.

Gurer-Orhan H., Ercal N., Mare S., Pennathur S., Orhan H., Heinecke Jay W. (2006): Misincorporation of free m-tyrosine into cellular proteins: A potential cytotoxic mechanism for oxidized amino acids. Biochemical Journal, 395: 277–284.

Haihua C., Qiming W., Zhuoran Z., Juntao K. (2023): Improvement of functional characteristics of *Hypophthalmichthys molitrix* protein by modification with chitosan oligosaccharide. Frontiers in Nutrition, 10: 1140191–1140191.

Jia G., Sha K., Feng X., Liu H. (2019): Post-thawing metabolite profile and amino acid oxidation of thawed pork tenderloin by HVEF-A short communication. Food Chemistry, 291: 16–21.

Jiang W., He Y., Xiong S., Liu Y., Yin T., Hu Y., You J. (2016): Effect of mild ozone oxidation on structural changes of silver carp (*Hypophthalmichthys molitrix*) myosin. Food and Bioprocess Technology, 10: 370–378.

Jin M., Xie Y., Xie P., Zheng Q., Wei T., Guo L., Lin J., Ye Z., Zou Y. (2022): Physicochemical and functional properties of *Pleurotus geesteranus* proteins. Food Research International, 162: 111978.

Juanjuan D., Jinxuan C., Changyu Z., Daodong P., Fang G., Ying W. (2022): Insight into the mechanism of myosin-fibrin gelation induced by non-disulfide covalent cross-linking. Food Research International, 156: 111168.

Kong D., Han R., Yuan M., Xi Q., Du Q., Li P., Yang Y., Applegate B., Wang J. (2023): Ultrasound combined with slightly acidic electrolyzed water thawing of mutton: Effects on physicochemical properties, oxidation and structure of myofibrillar protein. Ultrasonics Sonochemistry, 93: 106309.

Lei Y., Deng X., Zhang Z., Guo X., Zhang J. (2022): Effects of oxidation on the physicochemical properties and degradation of mutton myofibrillar proteins. Journal of Food Science, 87: 2932–2942.

Lepedda A.J., Formato M. (2020): Oxidative modifications in advanced atherosclerotic plaques: A focus on in situ protein sulfhydryl group oxidation. Oxidative Medicine and Cellular Longevity, 2020: 1–7.

Li C., He L., Ma S., Wu W., Yang H., Sun X., Peng A., Wang L., Jin G., Zhang J., Jin Y., Ma M. (2018): Effect of irradiation modification on conformation and gelation properties of pork myofibrillar and sarcoplasmic protein. Food Hydrocolloids, 84: 181–192.

Liu W., Ding H., Erdene K., Chen R., Mu Q., Ao C., Plaizier J. (2019): Effects of flavonoids from allium mongolicum regel as a dietary additive on meat quality and composition of fatty acids related to flavor in lambs. Canadian Journal of Animal Science, 99: 15–23.

Lu H., Luo Y., Lametsch R. (2018): Proteomic profiling of oxidized cysteine and methionine residues by hydroxyl radicals in myosin of pork. Food Chemistry, 243: 277–284.

Malik M.A., Sharma H.K., Saini C.S. (2017): High intensity ultrasound treatment of protein isolate extracted from dephenolized sunflower meal: Effect on physicochemical and functional properties. Ultrasonics Sonochemistry, 39: 511–519.

Márquez-Lázaro J.P., Mora L., Méndez-Cuadro D., Rodríguez-Cavallo E., Toldrá F. (2022): *In vitro* oxidation promoted by sarafloxacin antibiotic residues on myosin and

https://doi.org/10.17221/133/2024-CJFS

chicken meat proteins. Journal of Food Composition and Analysis, 111: 104622.

Menard L.M., Wood N.B., Vigoreaux J.O. (2021): Secondary structure of the novel myosin binding domain WYR and implications within myosin structure. Biology, 10: 603.

Nyaisaba B.M., Liu X., Zhu S., Fan X., Sun L., Hatab S., Miao W., Chen M., Deng S. (2019): Effect of hydroxyl-radical on the biochemical properties and structure of myofibrillar protein from Alaska pollock (*Theragra chalcogramma*). LWT – Food Science and Technology, 106: 15–21.

Potter J.D. (2022): Reprint of: The content of troponin, tropomyosin, actin, and myosin in rabbit skeletal muscle myofibrils. Archives of Biochemistry and Biophysics, 726: 109241.

Ramadhan A.H., Yu D., Jiang Q., Xu Y., Chen H., Wang L., Xia W. (2024): *In vitro* susceptibility of grass carp fish (*Ctenopharyngodon idella*) to oxidized myosin on structural change of protein secondary structure associated with reactive oxygen species (ROS) treatment. Food Bioscience, 60: 104319.

Shen H., Stephen Elmore J., Zhao M., Sun W. (2020): Effect of oxidation on the gel properties of porcine myofibrillar proteins and their binding abilities with selected flavour compounds. Food Chemistry, 329: 127032.

Shui S., Chen Y., Yan H., Song J., Liu S., Benjakul S., Zhang B. (2024): Comparative analyses of physicochemical and volatile flavor characteristics in hooked, trawl-net, and radar-net hairtail (*Trichiurus haumela*) muscles during long-term cryopreservation at −18 °C. Food Science & Nutrition, 12: 8159–8170.

Soladoye O.P., Juárez M.L., Aalhus J.L., Shand P., Estévez M. (2015): Protein oxidation in processed meat: Mechanisms and potential implications on human health. Comprehensive Reviews in Food Science and Food Safety, 14: 106–122.

Tong Q., Chen L., Wang W., Zhang Z., Yu X., Ren F. (2018): Effects of konjac glucomannan and acetylated distarch phosphate on the gel properties of pork meat myofibrillar proteins. Journal of Food Science and Technology, 55: 2899–2909.

Wu C., Wu F., Ju Q., Zhang Y., Yuan Y., Kang S., Hu Y., Luan G. (2023): The role of β-subunit in emulsifying performance of β-conglycinin. Food Hydrocolloids, 141: 108694.

Xinrong B., Huihui W., Yujiao W., Theodora O., Huaili N., Li Z., Qunli Y. (2023): Effects of iron-catalyzed oxidation and methemoglobin oxidation systems on endogenous enzyme activity and myofibrillar protein degradation in yak meat. Food Chemistry, 404: 134647.

Xu Y., Wang R., Zhao H., Yin Y., Li X., Yi S., Li J. (2020): Effect of heat treatment duration on the interaction between fish myosin and selected flavor compounds. Journal of the Science of Food and Agriculture, 100: 4457–4463.

Yantao Y., Lujuan X., Wangang Z. (2023): Moderate protein oxidation improves bovine myofibril digestibility by releasing peptides in the S2 region of myosin: A peptidomics perspective. Journal of Agricultural and Food Chemistry, 71: 2514–2522.

Ye Y., Chen F., Shi M., Wang Y., Xiao X., Wu C. (2024): Gel properties and protein structures of minced pork prepared with κ-carrageenan and non-meat proteins. Gels, 10: 305.

Yu S., Kuan Y.C., Chang C.-F., Liaw E.-T., Huang E.S., Lin J.-F., Chen Y.-K., Yu H.-S. (2023): The effect of papain hydrolysis on tropomyosin levels in shrimp. Heliyon, 9: e22410.

Zhang W., Xiao S., Ahn D.U. (2013): Protein oxidation: Basic principles and implications for meat quality. Critical Reviews in Food Science and Nutrition, 53: 1191–1201.

Zhang Y., Jamali M.A., Peng Z. (2019): Influence of salt substitute containing KCl, L-histidine and L-lysine on the secondary structure and gel properties of myosin. CyTA – Journal of Food, 17: 44–50.

Zhang D., Li H., Emara A.M., Hu Y., Wang Z., Wang M., He Z. (2020): Effect of *in vitro* oxidation on the water retention mechanism of myofibrillar proteins gel from pork muscles. Food Chemistry, 315: 126226.

Zhou Y., Yang H. (2020): Enhancing tilapia fish myosin solubility using proline in low ionic strength solution. Food Chemistry, 320: 12665.

Zhu C.Z., Jin H.Q., Yin F., Cui W.M., Zhang Q.H., Zhao G.M. (2021): Emulsion-forming properties of heat-induced pork myofibrillar protein affected by NaCl. International Journal of Food Science & Technology, 56: 3016–3025.

Received: July 3, 2024
Accepted: October 31, 2024
Published online: November 29, 2024